*Exp. Anim. 63(2), 193–204, 2014*

**—Original—**

# A New *Enpp1* allele, *Enpp1*$^{ttw\text{-}Ham}$, Identified in an ICR Closed Colony

Shuji TAKABAYASHI[1)], Shintaro SETO[2)], and Hideki KATOH[1)]

[1)]*Institute for Experimental Animals, Hamamatsu University School of Medicine, 1–20–1 Handayama, Higashi-ku, Hamamatsu, Shizuoka 431-3192, Japan*
[2)]*Department of Infectious Diseases, Hamamatsu University School of Medicine, 1–20–1 Handayama, Higashi-ku, Hamamatsu, Shizuoka 431-3192, Japan*

**Abstract:** We recently have reported on a novel ankylosis gene that is closely linked to the *Enpp1* (ectonucleotide pyrophosphatase/phosphodiesterase 1) gene on chromosome 10. Here, we have discovered novel mutant mice in a Jcl:ICR closed colony with ankylosis in the toes of the forelimbs at about 3 weeks of age. The mutant mice exhibited rigidity in almost all joints, including the vertebral column, which increased with age. These mice also showed hypogrowth with age after 16 weeks due to a loss of visceral fat, which may have been caused by poor nutrition. Histological examination and soft X-ray imaging demonstrated the ectopic ossification of various joints in the mutant mice. In particular, increased calcium deposits were observed in the joints of the toes, the carpal bones and the vertebral column. We sequenced all exons and exon/intron boundaries of *Enpp1* in the normal and mutant mice, and identified a G-to-T substitution (c.259+1G>T) in the 5′ splice donor site of intron 2 in the *Enpp1* gene of the mutant mice. This substitution led to the skipping of exon 2 (73 bp), which generated a stop codon at position 354 bp (amino acid 62) of the cDNA (p.V63Xfs). Nucleotide pyrophosphohydrolase (NPPH) activity of ENPP1 in the mutant mice was also decreased, suggesting that *Enpp1* gene function is disrupted in this novel mutant. The mutant mice reported in this study will be a valuable animal model for future studies of human osteochondral diseases and malnutrition.
**Key words:** Enpp1, pontaneous mutation, tiptoe walking (ttw)

## Introduction

The etiology of osteochondrodysplasia in human is still unclear, with pathological studies limited by the difficulty in obtaining lesions from patients with osteochondrodysplasia. As a consequence, the creation of animal models of human osteochondrodysplasia is desired. To date, several spontaneous mutant models and knock-out mice with osteochondrodysplasia-like diseases have been described. The tiptoe walking (*ttw*) mutant mouse is one such model of human ossification of the posterior longitudinal ligament of the spine (OPLL) disease [12, 15, 23, 39], which is caused by a nonsense mutation in the *Enpp1* gene [31].

Recently, we discovered an autosomal recessive gene causing ankylosis in a Jcl:ICR male mouse closely linked to the *Enpp1* gene on chromosome 10 [21]. Mice homozygous for this gene are characterized by tiptoe walking, stiffness of the vertebral column and limb joints, and progressive hypercalcification. These phenotypes are similar to those seen in the *Enpp1*$^{ttw\text{-}Jic}$ (synonymous to *ttw*) [10, 15] and *Enpp1* knock-out mice [18].

In this paper, we describe the phenotypes of the mutant mice homozygous for a new *Enpp1* allele from the

*(Received 25 October 2013 / Accepted 25 November 2013)*
*Address corresponding: S. Takabayashi, Institute for Experimental Animals, Hamamatsu University School of Medicine, 1–20–1 Handayama, Higashi-ku, Hamamatsu, Shizuoka 431-3192, Japan*

**Table 1.** Enpp1 sequencing primer sets used for genomic PCR (5′-3′)

| Exon no. | Forward primer | Reverse primer | Product size (bp) |
|---|---|---|---|
| 1 | GCCCGAAATCAGACAGGAAG | GAAGAGGACGGTATGTCAAGG | 522 |
| 2 | TCCAGAACAGGACATAAATCACAAG | CATAGGCACACATGCATCCAC | 306 |
| 3 | GAGTTACACTCCACAGTGGT | TTCCGGGAGATCTTTTCCTG | 314 |
| 4 | CCTGAAAATGGCTGCTGGAA | TGACATCACGTGTCCTTGGT | 597 |
| 5 | ATCCAGAGGTGGAGGATGAG | GCCAAGATGCTTTCTTCCGT | 582 |
| 6 | CAGTTGCATGCTGACCTCAA | AGTTCACCGCTTTGCAATGG | 383 |
| 7, 8 | TGCGATATGCCTAATAGCAG | CAGTTTGCCGAAATTCCTAC | 488 |
| 9 | TCTCTGTCTCCTTCGAGGTT | CTCTGGATGGCCTTCCATTC | 536 |
| 10, 11 | AAAGTTCTGCGTCAGTTTCC | AACTGTAAGCAAAGCCAGTT | 821 |
| 12 | CTCTGCCCTCTTTCCCTACA | TATGGCTGGCCATATCCACAA | 453 |
| 13 | GCAGATCTCTGTGAGCTCAAG | GCTACCCTCTCTTCACTCCA | 432 |
| 14 | TCCTAGAGTTGCAGGTAGGAG | AGCACAGTAGGACATCATGAC | 350 |
| 15 | CACTGTAACCCAGTGACACTC | TGAAGAACACCCTACACGTACT | 494 |
| 16 | CAGAGTAGGCATTCCAAGACC | ACTGTCGTTCTCTACACACTCA | 434 |
| 17 | TTGACCACCTCCATGCACAA | CACATGAGTGCTGGTGACAAC | 311 |
| 18 | CCCAGGTTCAGTTTCCAACA | TATACTCACCCAAGGGTCACA | 515 |
| 19 | AATTGCTGCTTCTCCTCTTCC | AGGCATACCTTTCACAAACCAG | 444 |
| 20 | CATGAGTGCTCCGTTGTAGAG | AGGCAGATTTCTGAGTTTGAGG | 517 |
| 21 | CATGACGATTGCCCCTAAC | ATTTGGTGCTGACACTTGG | 366 |
| 22 | TGTTACTCTCCACCCCAAGA | GCACCAAAGAAGCACAAACC | 629 |
| 23 | ATACCATTCGCCAGTTCCAC | ATCTACACAGGGCTCACGA | 431 |
| 24 | CAGTGTTTCTCTGTGTAGAACAGG | GTTTCTTCCAGAGTGTGAGCAA | 489 |
| 25 | CGTGAACTGAGTGCTCTCTG | ATGAGCTACCCCAGTCCTT | 601 |

Jcl:ICR closed colony. We also describe the mutation of the new *Enpp1* allele that differs from that of the *Enpp1*$^{ttw\text{-}Jic}$ mutation based on the sequence data.

## Materials and Methods

*Mice*

Jcl:ICR, BALB/cByJJcl, C57BL/6JJcl, C3H/HeJJcl and DBA/2JJcl mice were purchased from CLEA Japan (Tokyo, Japan). A novel mutation causing ankylosis was carried by the Jcl:ICR #48 male mouse [21]. A congenic strain carrying *Enpp1*$^{ttw\text{-}Ham}$ was generated by backcrossing to transfer the ankylotic responsible gene into the C57BL/6JJcl strain. Mice used for phenotypic analyses were over the N12 generation. Male and female mice were housed separately in plastic cages lined with sterilized wood shavings in a room with a constant temperature (24–26°C) and with a constant light cycle (12 h light/dark). A solid diet (LabDiet; PMI Nutrition International, St. Louis, MO, USA) and water were provided *ad libitum*.

This study was approved by the Hamamatsu University School of Medicine Animal Care and Use Committee.

*Measurement of body weight, organ weight and food intake*

Each of the mutant and normal mice were separated in a cage for 24 h. Body weight was measured once per week using an electronic balance. Mutant and normal mice were sacrificed at 16 and 20 weeks of age and the weights of their organs and visceral fat were measured using an electronic balance. Food intake (g/day/mouse) was examined by deducting the remaining and the spilled feed amount from the provided feed amount. Food intake was measured at 8, 12 and 16 weeks of age.

*Measurement of nucleotide pyrophosphohydrolase (NPPH) activity*

Blood was taken from the intraorbital sinuses of 16-week-old mutant and normal mice using a heparinized capillary under free-feeding conditions. The plasma obtained by centrifugation was preserved at −80°C. Plasma NPPH was measured according to a colorimetric assay [7]. Briefly, reagents were prepared in a plastic microcentrifuge tube, as follows: 10 $\mu$l of plasma sample diluted in 90 $\mu$l of 10 mM Tris-HCl buffer (pH 7.8) was added to an equal volume of 2 mM thymidine monophosphate paranitrophenyl ester (TMPNP) (Sigma-Aldrich, St. Louis, MO, USA) in 50 mM sodium carbonate buffer (pH 9.8). The prepared sample was incubated for 1 h at 37°C. The reaction was stopped by the addition of

0.1 N NaOH, and the absorbance was determined at 405 nm in a spectrophotometer (BioRad, Hercules, CA, USA).

*Grip strength test*

All mice were subjected to the grip strength test in order to discriminate the mutant mice from the normal mice. Briefly, mice were put on wired mesh and pulled backward. Grip strength was evaluated by the investigator according to the methods previously reported [35].

*Morphological and histological analyses*

The mutant and normal mice were subjected to a soft X-ray (Softex-C-60, SOFTEX Co., Ltd., Kanagawa, Japan) in order to observe the morphological condition of the various joints.

Vertebral columns of the mutant and normal mice were dissected and fixed in 10% neutral buffered formalin for 24 h, then decalcified with Plank-Rychlo's solution (Wako, Osaka, Japan). After decalcification, the vertebral columns were bisected sagittally in the median plane. The tissues were then embedded in paraffin and sectioned into 4 $\mu$m-thick sections. Histological examination was performed after staining with Hematoxylin and Eosin (H&E).

For skeletal preparations, the skin and viscera of the mutant and normal mice were removed, and the samples fixed in 95% ethanol overnight, followed by staining with 0.01% alcian blue and 0.015% alizarin red for the cartilage and bone, respectively. The samples were destained with 1% KOH solution and then subsequently treated in 20%, 40%, 60% and 80% (v/v) glycerol solutions prepared in 1% KOH. Cleared samples were stored in 100% glycerol.

*Sequencing of the Enpp1 gene*

The entire coding region of mutant and normal mice, corresponding to exons 1–25 of the *Enpp1* gene, were amplified using the 23 primer pairs listed in Table 1. Nucleotide sequences of these primers were determined from the Ensembl database (http://www.ensembl.org/Mus_musculus/index.html). These primers were used to amplify genomic DNA according to the methods previously reported [43].

PCR products were sequenced directly using the dideoxy chain-termination method with a BigDye Terminator v3.1 Cycle Sequencing kit (Life technologies, Carisbad, CA, USA), and then applied to an automated DNA sequencer ABI3100 (Life technologies).

*PCR-RFLP*

PCR products amplified using the Exon2 primer set (Table 1) were digested with a restriction endonuclease, *Pac*I at 37°C for 1 h, and then electrophoresed on a 3% agarose gel, according to the method previously reported [44].

*RT-PCR*

Total RNA was isolated from the forelimbs and kidneys using an RNeasy kit (Qiagen, Germantown MD, USA) according to the manufacturer's instructions. Total RNA (1 $\mu$g) was reverse transcribed using oligo-dT primer and superscript II RT (Life technologies). cDNA was amplified using Enpp1-RT primers (5′-CCAAAGACCCCAACACCTAC-3′ and 5′-CGCACCTGAATTTGTTGC-3′), and RT-PCR products were electrophoresed and sequenced according to the method previously reported [42].

*Statistical analysis*

Statistical analyses were performed using Prism5 software (GraphPad software, San Diego, CA, USA). All data were expressed as mean ± standard deviation (SD). Differences between mutant and normal measures were analyzed using Student's *t* test. Survival data were analyzed with Kaplan–Meier analysis, with the *P* values derived from the Mantel–Cox Log-rank statistic. *P* value <0.05 was judged as significant.

## Results

*Body weight and food intake*

Kaplan-Meier analysis of the probability of survival of the mice with age is shown in Fig. 1A. Survival differences began to appear relative to normal controls in the mutant group at around 100 days of age, with all mutant mice dead by 220 days of age with a median survival of 118 days (normal vs. mutant Kaplan-Meier Mantel-Cox: $P<0.0001$).

Mutant mice gained body weight at the same rate as normal mice up to 4 and 8 weeks of age. However, mutant mice were significantly lighter than normal mice at 12, 16 and 20 weeks: 20.9 ± 0.5 g vs. 25.0 ± 0.6 g, 20.7 ± 0.8 g vs. 27.5 ± 0.6 g, and, 17.3 ± 0.8 g vs. 27.2 ± 0.7 g, respectively (Fig. 1B).

Similarly, there was no significant difference in the

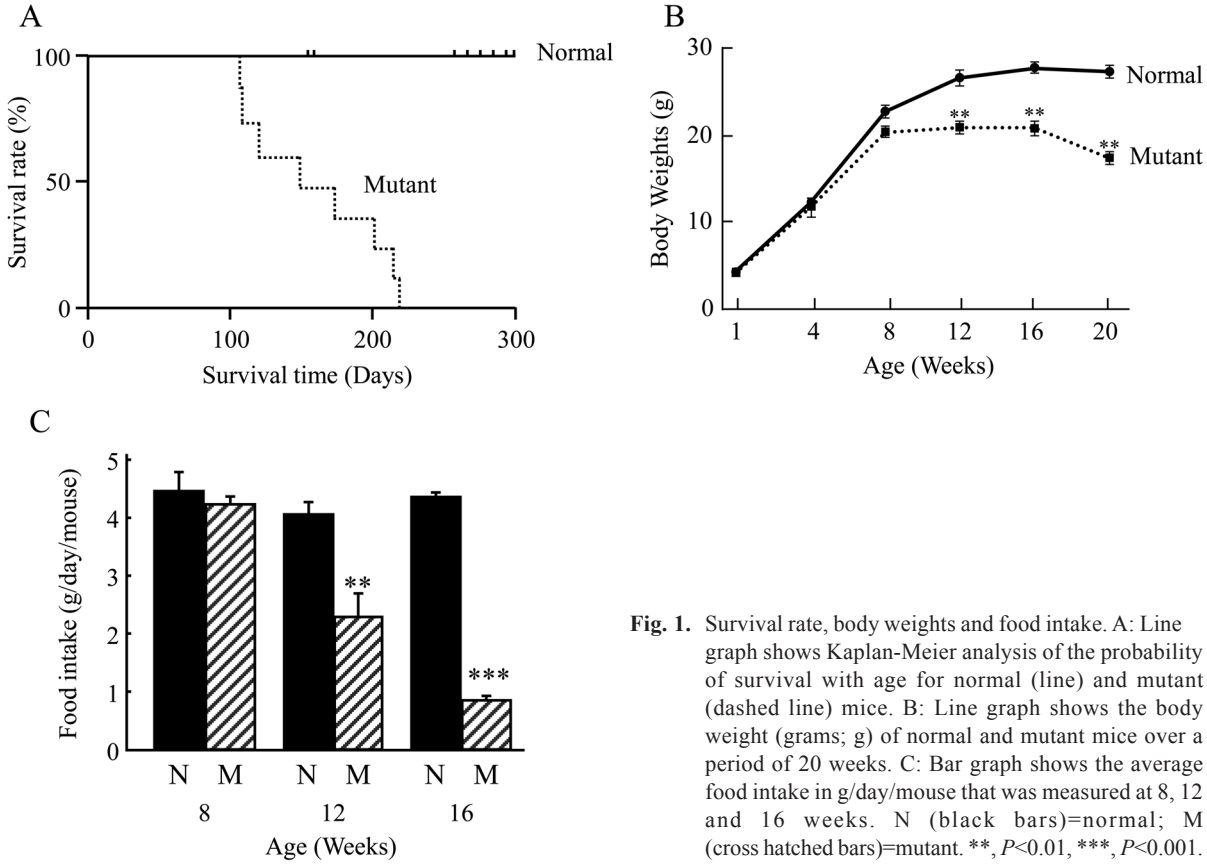


**Fig. 1.** Survival rate, body weights and food intake. A: Line graph shows Kaplan-Meier analysis of the probability of survival with age for normal (line) and mutant (dashed line) mice. B: Line graph shows the body weight (grams; g) of normal and mutant mice over a period of 20 weeks. C: Bar graph shows the average food intake in g/day/mouse that was measured at 8, 12 and 16 weeks. N (black bars)=normal; M (cross hatched bars)=mutant. **, $P<0.01$, ***, $P<0.001$.

food intake of the mutant and normal mice at 8 weeks of age (Fig. 1C). However, food intake of the mutant mice was significantly decreased at 12 and 16 weeks as compared with the normal mice at the same age.

In the mutant mice, the average weight of visceral fat reduced sharply with age. By comparison, the weight of visceral fat in the normal mice were maintained substantially constant with age (Fig. 2A). In addition, at 16 weeks of age, the average size of the adipocytes was smaller in the mutant mice than in the normal mice (Fig. 2B).

*Morphology of the mutant mice*

At 3 weeks of age, the mutant mice showed stiffness in the toes of their forelimbs, but not in their hindlimbs. This phenotypic abnormality was confirmed by the grip strength test. After weaning, the mutant mice exhibited tiptoe walking due to progressive ankylosis of the forelimbs with aging. As shown in Fig. 3, in 12-week-old mutant mice, calcification was observed in and around the forelimb joints, and ectopic ossification was detected in the carpal bones.

The mutant mice also showed rigidity in almost all movable joints with aging, including the vertebral column. At 8 weeks of age, soft X-ray examination showed similar vertebral borders in both the normal and mutant mice (Figs. 4A1 and B1). However, by 18 weeks of age, progressive hypercalcification was observed in the mutant mice (Figs. 4A3 and B3), with marked deposition of calcium in the intervertebral spaces, especially at both edges of the vertebral bodies (Fig. 4B3).

Using H&E staining, histological examination revealed degeneration and destruction of the cartilage matrix and lateral protrusion in the intervertebral discs of the mutant mice by as early as 8 weeks of age. These protruded discs occasionally pressed onto the spinal cord (Fig. 4B2). The volume of the nucleus pulposus in the intervertebral discs of the mutant mice increased with age, causing herniation into the anterior and posterior regions (Fig. 4B4). Endochondral ossification was observed in the cartilaginous cells in the protruded and ruptured annulus fibrosus as well as in the anterior and

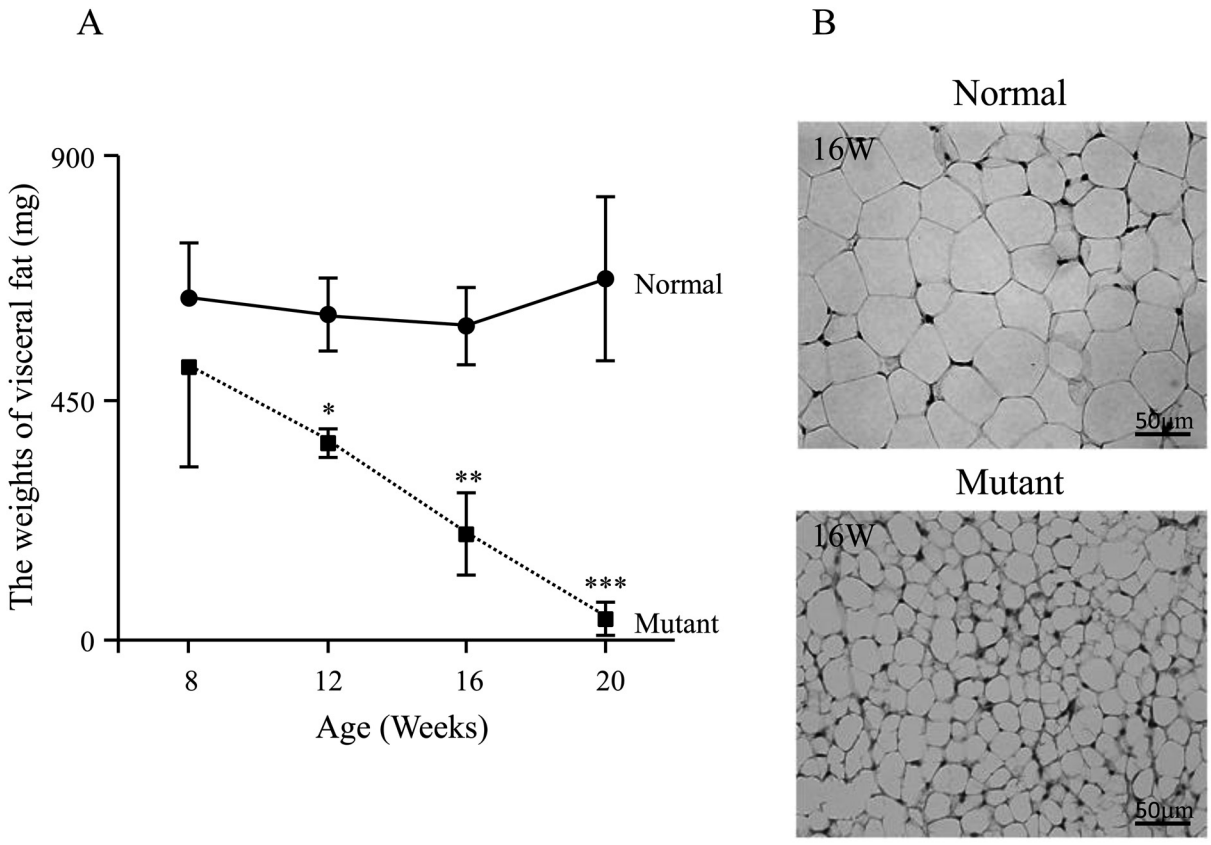


**Fig. 2.** Visceral fat and adipocyte characteristics. The graph illustrates the weight (mg) of visceral fat in the mice at the 16 and 20 week (W) time points (A). Adipocyte at 16 weeks (W) for normal and mutant mice. Scale bar represents 50 $\mu$m (B). *, $P<0.05$, **, $P<0.01$, ***, $P<0.001$.

posterior longitudinal ligaments at 18 weeks of age (Fig. 4B4). Ectopic ossifications of the ear cartilages and whisker follicles were also observed on soft X-ray films at 18 weeks of age (data not shown).

*Sequencing*

All exons, including exon/intron boundaries, of the mutant and normal mice were sequenced using genomic PCR, followed by direct DNA sequencing. The sequences of *Enpp1* coding regions were identical in the normal and mutant mice. However, a G-to-T substitution was observed in the splice donor site (c.259+1G>T) at the exon/intron boundary of exon 2 in the mutant mice (Fig. 5A). Since an abnormal transcript of *Enpp1* was predicted in the mutant mice, we performed RT-PCR and direct sequencing using primers spanning the last 36 bp of exon 1 and the first 33 bp of exon 4 (Fig. 5B). As shown in Fig. 5C, a normal PCR product (259 bp) corresponding to the expected sequence of *Enpp1* cDNA was amplified in the normal mice, but an abnormal PCR product (186 bp), shorter by 73 bp, was amplified in the mutant mice. The deletion of exon 2 led to this frame shift by creating a stop codon (TAA) at the first codon of exon 3 (p.V63Xfs) (Fig. 5B). We performed western blot analysis in kidney lysate of normal and mutant mouse using the anti-ENPP1 antibody (Everest Biotech, Oxfordshire, UK). But, we failed to detect ENPP1 proteins even in normal lysate (data not shown). Since the nucleotide substitution generated a *Pac* I restriction site, we digested the PCR products with the restriction enzyme. As expected, two bands (254 bp and 54 bp) were observed in the mutant mice after digestion (Fig. 5D). To exclude the possibility that this mutation was merely a genetic polymorphism, we applied PCR-RFLP analysis to common inbred strains, BALB/cByJJcl, C57BL/6JJcl, C3H/HeJJcl, DBA/2JJcl and 40 Jcl:ICR mice colonies, including Jcl:ICR #48. As expected, the mutation was not observed in the inbred strains and ICR

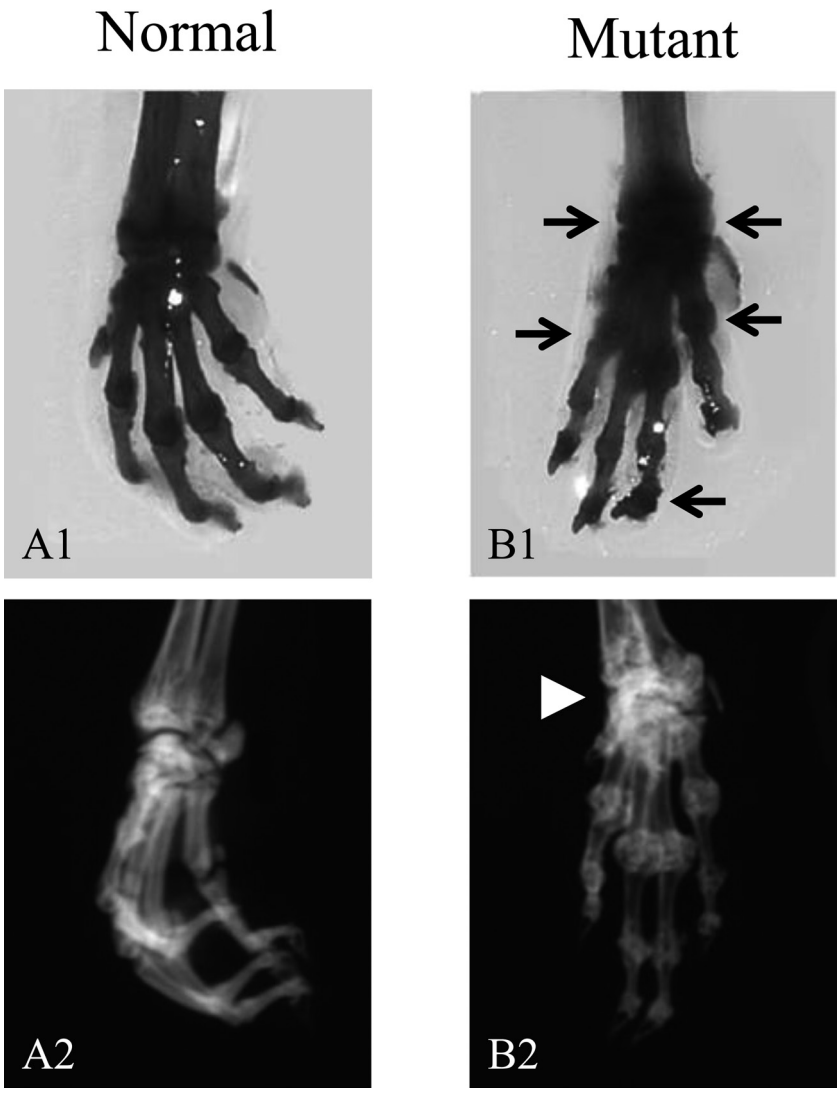


**Fig. 3.** Forelimb malformation in 12-week-old mice. Alcian blue stains cartilage and alizarin red stains ossified bone (A1 and B1). Mutant forelimb show ectopic ossification (arrows) (B1). Soft X-ray (A2 and B2) Calcification was observed in and around the forelimb joints, and ectopic ossification was detected in the carpal bones (arrowhead) in the mutant mice (B1 and B2).

individuals, with the exception of Jcl:ICR #48. Thus, this mutation in the *Enpp1* gene seems likely to be the cause of the progressive ankylosis. Hereafter, this novel mutation is referred as to *Enpp1*$^{ttw\text{-}Ham}$, in accordance with international nomenclature.

*NPPH activity*

ENPP1 is a membrane-bound ectoenzyme with alkaline phosphodiesterase I and have NPPH activities [33]. To confirm the enzyme activity of Enpp1$^{ttw\text{-}Ham}$ protein, we measured the plasma NPPH activity. The NPPH activity of the *Enpp1*$^{ttw\text{-}Ham}$ mutant mice was 20.4% that of the activity in normal mice (100%). In mice heterozygous for *Enpp1*$^{ttw\text{-}Ham}$, the activity was the same (99.7%) as that of the normal mice (data not shown).

## Discussion

We have found a novel recessive gene causing ankylosis in a Jcl:ICR closed colony, which is synonymous with outbred stock. The gene responsible was mapped to chromosome 10 [21]. In this study, we performed

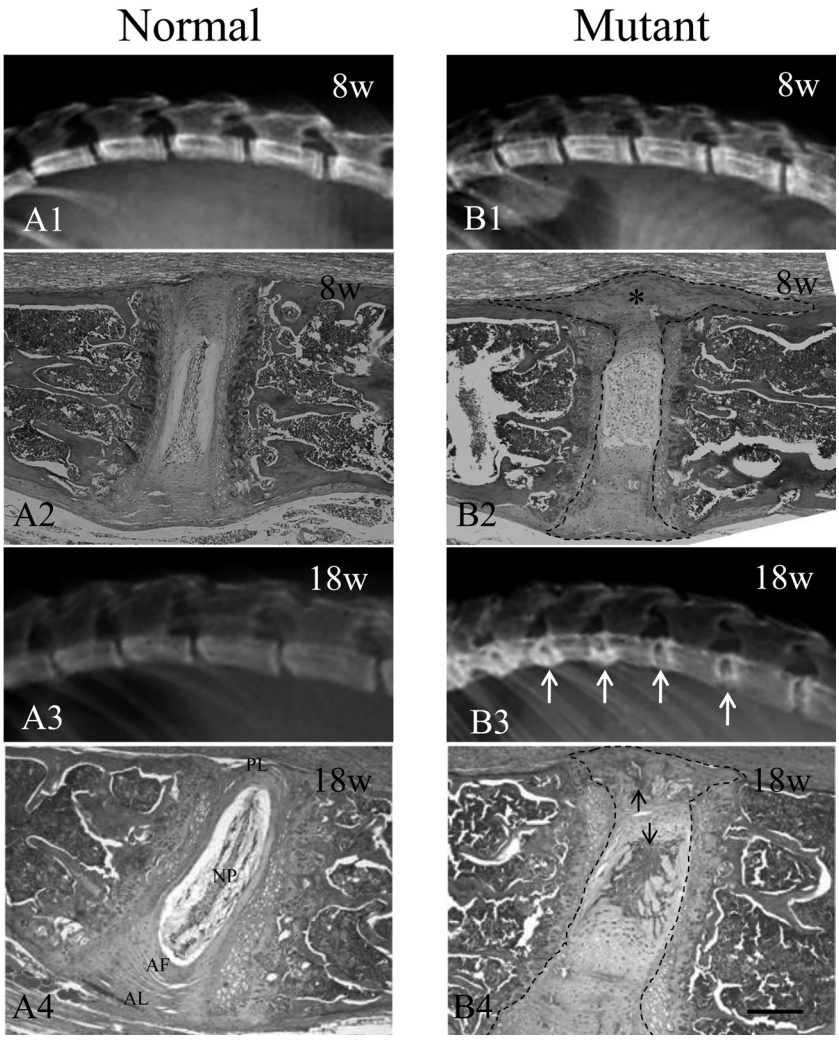


**Fig. 4.** Phenotypes of vertebral columns of normal and mutant mice. Soft X-ray film of the mutant and normal mice (A1, A3, B1 and B3). The mutant mice showing deposition of calcium in the intervertebral discs (white arrows). H&E staining of the vertebral columns of mutant and normal mice (A2, A4, B2 and B4). Histological examination revealed cartilage degeneration and lateral protrusion in the intervertebral discs (asterisk) in 8-week-old mutant mice (B2) as compared with normal mice (A2). Lesions are outlined with black dash lines (B2). Endochondral ossification was observed in the cartilaginous cells in the protruded and ruptured annulus fibrosus as well as in the anterior and posterior longitudinal ligaments at 18 weeks in the mutant mice (black arrows, B4) as compared with the normal mice at the same time point (A4). Lesions are outlined with black dash lines (B4). AF, annulus fibrosus. AL, anterior longitudinal ligament. NP, nucleus pulposus. PL, posterior longitudinal ligament. Scale bar represents 200 $\mu$m.

sequencing in order to demonstrate that this genetic mutation caused ankylosis. Our sequence data of the *Enpp1* gene in the mutant mice revealed a splice donor site mutation (G-to-T) at the exon 2/intron 2 boundary (c.259+1G>T) of the *Enpp1* gene. Exon 2 skipping resulted in the creation of a stop codon TAA at the first codon of exon 3 at amino acid position 62 (p.V63Xfs).

Splice acceptor site or donor site mutations with exon skipping have been reported occasionally [13, 38], and several genetic diseases may be the result of splice site mutations [4, 38]. Unless base pairs are removed in multiples of three, the mutation causes a frame-shift and

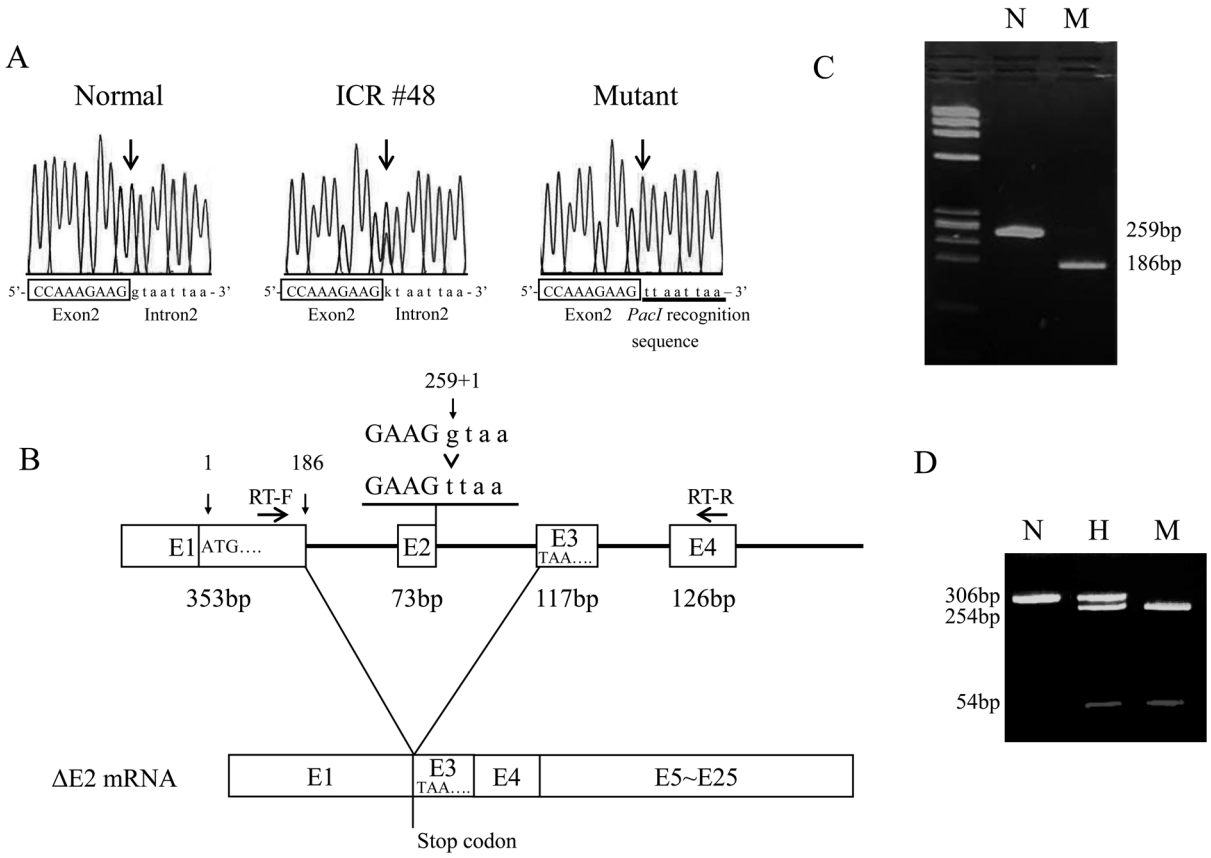


**Fig. 5.** Nucleotide sequencing of the *Enpp1* gene. A: Sequencing of the normal, Jcl:ICR #48 and mutant mouse samples. Arrows in chromatograms show the G to T nucleotide substitution at the splice donor site. B: RT-PCR analysis for normal (N) and mutant (M) littermates. The wild-type allele yielded a 259 bp fragment and the mutant allele yielded a 186 bp fragment. C: A schematic of the predicted mutant mRNA. Arrows show primers for RT-PCR. D: PCR-RFLP analysis for normal (N), heterozygous (H) and mutant (M) littermates using *PacI* restriction enzyme to digest genomic PCR products. The wild-type allele yielded a single 306 bp fragment, whereas the mutant allele yielded two fragments of 254 bp and 54 bp.

results in the generation of an abnormal protein.

The *Enpp1*$^{ttw\text{-}Jic}$ mutation was discovered as *twy* (tip-toe walking Yoshimura) during brother-sister mating which was performed to establish a series of inbred strains from genetically heterogeneous Jcl:ICR closed colony mice at the central Institute for Experimental Animals in 1978 [15]. Okawa *et al.* (1998) demonstrated that the *Enpp1*$^{ttw\text{-}Jic}$ has a single nucleotide substitution (c.1702G>T) causing a nonsense mutation (p.G568X) halfway through the coding region of ENPP1 (Fig. 6) [31]. The morphological features of the *Enpp1*$^{ttw\text{-}Jic}$ mice have since been reported in numerous papers [2, 12, 15, 23, 32, 39]. Recently, *Enpp1* knock-out mice and *N*-ethyl-*N*-nitrosourea (ENU)-induced *Enpp1* mutant mice have also been reported [3]. Overall, the phenotypes of *Enpp1* mutant mice reported to date are very similar to one another. Moreover, no apparent effects of the genetic background on the mutant phenotypes have been observed.

Studies have shown that ENPP1 inhibits insulin signaling [9], and ENPP1 overexpression is associated with type 2 diabetes and obesity in humans [1, 6]. In this paper, we described the weight loss and the adipocyte abnormality in the *Enpp1*$^{ttw\text{-}Ham}$ mice; however, we detected no differences in blood insulin levels between the mutant and normal littermates (data not shown). The weight loss may be attributed to the decreased food intake in the *Enpp1*$^{ttw\text{-}Ham}$ mice.

ENPP1 is a type II transmembrane metalloenzyme characterized by a modular structure composed of a short intracellular domain, a single transmembrane domain and an extracellular domain containing a conserved catalytic site [5, 45]. The mutation observed in this study may lead to a premature truncation of the protein prod-

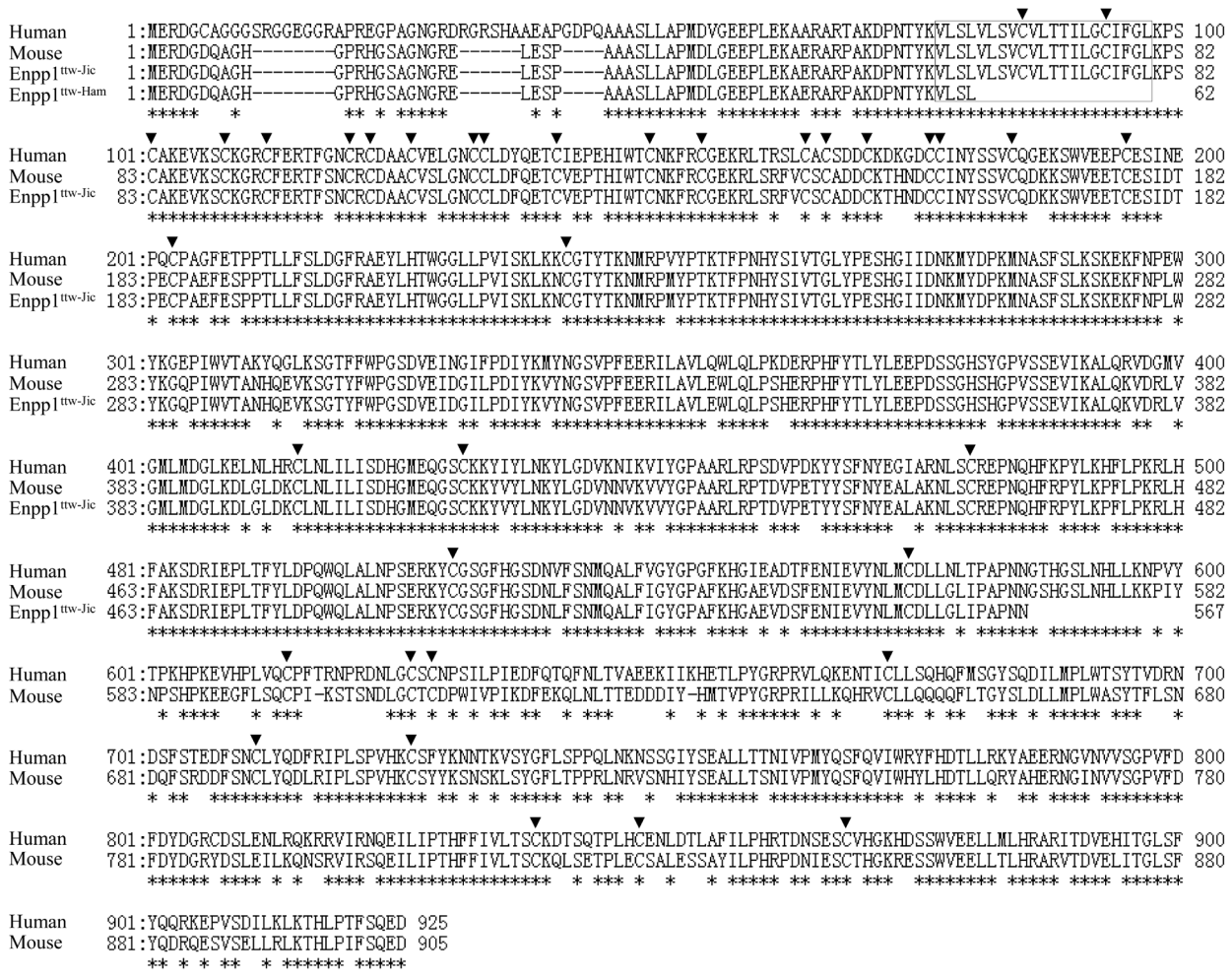


**Fig. 6.** Predicted amino acid sequence of Enpp1$^{ttw\text{-}Ham}$ compared with the known human, mouse, and Enpp1$^{ttw\text{-}Jic}$ sequences, as shown. Enpp1$^{ttw\text{-}Ham}$ and Enpp1$^{ttw\text{-}Jic}$ mutations are Val63stop and Gly568stop, respectively. The amino acid sequence homology is 78.8% between mouse and human. The transmembrane region is boxed. Arrowheads indicate conserved cysteine residues. Asterisks indicate amino acid identity between human and mouse.

uct that lacks a portion of the cysteine-rich region which contains both the calcium binding domain and the cysteine residues used in disulfide bonding (Fig. 6).

ENPP1 has NPPH activity that generates inorganic pyrophosphate (PPi) [7]. PPi is a potent inhibitor of hydroxyapatite mineralization because it antagonizes the ability of inorganic phosphate (Pi) to crystalize with $Ca^{2+}$ to form hydroxyapatite [11, 28]. PPi regulates mineralized tissue development and the decrease in PPi causes pathologic calcification [31, 39]. Our results demonstrated a lack of NPPH activity in the mutant mice: this suggests that *Enpp1* gene function is completely disrupted in this novel mutant and then the mutant mice have ectopic ossification and ankylosis.

ENPP1 is highly conserved amino acid sequence in human and mouse. The amino acid sequence homology is 78.8% between mouse and human (Fig. 6). In humans, ENPP1 mutations have been associated with several disorders including idiopathic infantile arterial calcification (IIAC) [36, 37], autosomal recessive hypophosphatemic rickets (ARHR) [25, 38] and OPLL of spine [29, 38]. The *Enpp1$^{ttw\text{-}Jic}$* mice are commonly known as a mouse model for human OPLL [12, 15, 23, 39]. OPLL is characterized by ectopic ossification of ligamentous tissues of the spine often leads to various degrees of myeloradiculopathy as a result of chronic pressure on the spinal cord and nerve roots [40, 41]. Our novel mutant revealed ectopic ossification of ligamentous tissues of the spine and the compression of the spinal cord. Those phenotypes closely resembled OPLL symptoms.

Although it is unclear whether novel *Enpp1*$^{ttw\text{-}Ham}$ mutant is useful as animal models for other ENPP1 associated disorders, including IIAC and ARHR, this mutant is a good animal model for the functional analysis of *ENPP1* gene.

There are many genes reported to be associated with OPLL in human, including ENPP1 [24, 29], collagen 6A1 [27], transforming growth factor-β (TGFB) -1 [20], TGFB-3 [30], collagen 11A2 [22], bone morphogenetic protein (BMP)-2 [46], RUNX2 [26], Fibroblast Growth factor 2 [19], BMP-9 [34], TGFB receptor type 2 [17], vitamin K epoxide reductase complex subunit 1 [8], however, the pathogenesis of OPLL remains to be elucidated. The expression analysis of OPLL related genes in *Enpp1* mutant mice might be contributory to understanding the pathogenesis of OPLL. In fact, several studies have reported an increase in Runx2 [16] and collagen 11 expression, [14] in OPLL-like region of *Enpp1*$^{ttw\text{-}Jic}$ mice.

Spontaneous, knock-out and chemically-induced mutations of the *Enpp1* gene have been reported. The *Enpp1*$^{ttw\text{-}Ham}$ mice reported in this study will be a valuable tool for the future studies of human osteochondral diseases, malnutrition and investigating the role of ENPP1 in other human disorders.

## Acknowledgments

We thank Jiro Kimura, Daisuke Ogasawara and Hiroki Uozaki for their technical assistance.

## References

1. Abate, N., Chandalia, M., Satija, P., Adams-Huet, B., Grundy, S.M., Sandeep, S., Radha, V., Deepa, R., and Mohan, V. 2005. ENPP1/PC-1 K121Q polymorphism and genetic susceptibility to type 2 diabetes. *Diabetes* 54: 1207–1213. [Medline] [CrossRef]
2. Baba, H., Furusawa, N., Fukuda, M., Maezawa, Y., Imura, S., Kawahara, N., Nakahashi, K., and Tomita, K. 1997. Potential role of streptozotocin in enhancing ossification of the posterior longitudinal ligament of the cervical spine in the hereditary spinal hyperostotic mouse (*twy*/*twy*). *Eur. J. Histochem*. 41: 191–202. [Medline]
3. Babij, P., Roudier, M., Graves, T., Han, C.Y., Chhoa, M., Li, C.M., Juan, T., Morony, S., Grisanti, M., Li, X., Yu, L., Dwyer, D., Lloyd, D.J., Bass, M.B., Richards, W.G., Ebeling, C., Amato, J., and Carlson, G. 2009. New variants in the Enpp1 and Ptpn6 genes cause low BMD, crystal-related arthropathy, and vascular calcification. *J. Bone Miner. Res*. 24: 1552–1564. [Medline] [CrossRef]
4. Bank, A., Dobkin, C., Donovan-Peluso, M., and Young, K. 1985. Abnormal globin gene structure and expression in beta-thalassemia. *Ann. N.Y. Acad. Sci*. 445: 1–9. [Medline] [CrossRef]
5. Belli, S.I., van Driel, I.R., and Goding, J.W. 1993. Identification and characterization of a soluble form of the plasma cell membrane glycoprotein PC-1 (5′-nucleotide phosphodiesterase). *Eur. J. Biochem*. 217: 421–428. [Medline] [CrossRef]
6. Bochenski, J., Placha, G., Wanic, K., Malecki, M., Sieradzki, J., Warram, J.H., and Krolewski, A.S. 2006. New polymorphism of ENPP1 (PC-1) is associated with increased risk of type 2 diabetes among obese individuals. *Diabetes* 55: 2626–2630. [Medline] [CrossRef]
7. Cardenal, A., Masuda, I., Haas, A.L., Ono, W., and McCarty, D.J. 1996. Identification of a nucleotide pyrophosphohydrolase from articular tissues in human serum. *Arthritis Rheum*. 39: 252–256. [Medline] [CrossRef]
8. Chin, D.K., Han, I.B., Ropper, A.E., Jeon, Y.J., Kim, D.H., Kim, Y.S., Park, Y., Teng, Y.D., Kim, N.K., and Kuh, S.U. 2013. Association of VKORC1-1639G>A polymorphism with susceptibility to ossification of the posterior longitudinal ligament of the spine: a Korean study. *Acta. Neurochir (Wien)*. 155: 1937–1942. [Medline] [CrossRef]
9. Costanzo, B.V., Trischitta, V., Di Paola, R., Spampinato, D., Pizzuti, A., Vigneri, R., and Frittitta, L. 2001. The Q allele variant (GLN121) of membrane glycoprotein PC-1 interacts with the insulin receptor and inhibits insulin signaling more effectively than the common K allele variant (LYS121). *Diabetes* 50: 831–836. [Medline] [CrossRef]
10. Esaki, K., Yoshimura, Y., and Katoh, H. 1990. Tip-toe walking (*ttw*). *Mouse Genome* 86: 242.
11. Fleisch, H. and Bisaz, S. 1962. Mechanism of calcification: inhibitory role of pyrophosphate. *Nature* 195: 911. [Medline] [CrossRef]
12. Furusawa, N., Baba, H., Imura, S., and Fukuda, M. 1996. Characteristics and mechanism of the ossification of posterior longitudinal ligament in the tip-toe walking Yoshimura (*twy*) mouse. *Eur. J. Histochem*. 40: 199–210. [Medline]
13. Hayashi, S., Kunisada, T., Ogawa, M., Yamaguchi, K., and Nishikawa, S. 1991. Exon skipping by mutation of an authentic splice of *c-kit* gene in *W*/*W* mouse. *Nucleic Acids Res*. 19: 1267–1271. [Medline] [CrossRef]
14. Hirakawa, H., Kusumi, T., Nitobe, T., Ueyama, K., Tanaka, M., Kudo, H., Toh, S., and Harata, S. 2004. An immunohistochemical evaluation of extracellular matrix components in the spinal posterior longitudinal ligament and intervertebral disc of the tiptoe walking mouse. *J. Orthop. Sci*. 9: 591–597. [Medline] [CrossRef]
15. Hosoda, Y., Yoshimura, Y., and Higaki, S. 1981. A new breed of mouse showing multiple osteochondral lesions-twy mouse. *Ryumachi* 21: 157–164. [Medline]
16. Iwasaki, M., Piao, J., Kimura, A., Sato, S., Inose, H., Ochi, H., Asou, Y., Shinomiya, K., Okawa, A., and Takeda, S. 2012. Runx2 haploinsufficiency ameliorates the development of ossification of the posterior longitudinal ligament. *PLoS ONE* 7: e43372. [Medline] [CrossRef]
17. Jekarl, D.W., Paek, C.M., An, Y.J., Kim, Y.J., Kim, M., Kim, Y., Lee, J., and Sung, C.H. 2013. TGFBR2 gene polymor-

phism is associated with ossification of the posterior longitudinal ligament. *J. Clin. Neurosci*. 20: 453–456. [Medline] [CrossRef]
18. Johnson, K., Goding, J., Van Etten, D., Sali, A., Hu, S.I., Farley, D., Krug, H., Hessle, L., Millan, J.L., and Terkeltaub, R. 2003. Linked deficiencies in extracellular PPi and osteopontin mediate pathologic calcification associated with defective PC-1 and ANK expression. *J. Bone Miner. Res*. 18: 994–1004. [Medline] [CrossRef]
19. Jun, J.K. and Kim, S.M. 2012. Association study of fibroblast growth factor 2 and fibroblast growth factor receptors gene polymorphism in korean ossification of the posterior longitudinal ligament patients. *J. Korean Neurosurg. Soc*. 52: 7–13. [CrossRef]
20. Kamiya, M., Harada, A., Mizuno, M., Iwata, H., and Yamada, Y. 2001. Association between a polymorphism of the transforming growth factor-beta 1 gene and genetic susceptibility to ossification of the posterior longitudinal ligament in Japanese patients. *Spine* 26: 1264–1267. [Medline] [CrossRef]
21. Katoh, H., Nishikawa, T., Kimura, J., Yamauchi, Y., and Takabayashi, S. 2010. Phenotype-based search of natural mutations related to hereditary diseases existing in a closed colony of mice. *Exp. Anim*. 59: 183–190. [Medline] [CrossRef]
22. Kong, Q., Ma, X., Li, F., Guo, Z., Qi, Q., Li, W., Yuan, H., Wang, Z., and Chen, Z. 2007. COL6A1 polymorphisms associated with ossification of the ligamentum flavum and ossification of the posterior longitudinal ligament. *Spine* 32: 2834–2838. [Medline] [CrossRef]
23. Koshizuka, Y., Ikegawa, S., Sano, M., Nakamura, K., and Nakamura, Y. 2001. Isolation of novel mouse genes associated with ectopic ossification by differential display method using *ttw*, a mouse model for ectopic ossification. *Cytogenet. Cell Genet*. 94: 163–168. [Medline] [CrossRef]
24. Koshizuka, Y., Kawaguchi, H., Ogata, N., Ikeda, T., Mabuchi, A., Seichi, A., Nakamura, Y., Nakamura, K., and Ikegawa, S. 2002. Nucleotide pyrophosphatase gene polymorphism associated with ossification of the posterior longitudinal ligament of the spine. *J. Bone Miner. Res*. 17: 138–144. [Medline] [CrossRef]
25. Levy-Litan, V., Hershkovitz, E., Avizov, L., Leventhal, N., Bercovich, D., Chalifa-Caspi, V., Manor, E., Buriakovsky, S., Hadad, Y., Goding, J., and Parvari, R. 2010. Autosomal-recessive hypophosphatemic rickets is associated with an inactivation mutation in the *ENPP1* gene. *Am. J. Hum. Genet*. 86: 273–278. [Medline] [CrossRef]
26. Liu, Y., Zhao, Y., Chen, Y., Shi, G., and Yuan, W. 2010. RUNX2 polymorphisms associated with OPLL and OLF in the Han population. *Clin. Orthop. Relat. Res*. 468: 3333–3341. [Medline] [CrossRef]
27. Maeda, S., Koga, H., Matsunaga, S., Numasawa, T., Ikari, K., Furushima, K., Harata, S., Takeda, J., Sakou, T., Komiya, S., and Inoue, I. 2001. Gender-specific haplotype association of collagen alpha 2 (XI) gene in ossification of the posterior longitudinal ligament of the spine. *J. Hum. Genet*. 46: 1–4. [Medline] [CrossRef]
28. Meyer, J.L. 1984. Can biological calcification occur in the presence of pyrophosphate? *Arch. Biochem. Biophys*. 231: 1–8. [Medline] [CrossRef]
29. Nakamura, I., Ikegawa, S., Okawa, A., Okuda, S., Koshizuka, Y., Kawaguchi, H., Nakamura, K., Koyama, T., Goto, S., Toguchida, J., Matsushita, M., Ochi, T., Takaoka, K., and Nakamura, Y. 1999. Association of the human NPPS gene with ossification of the posterior longitudinal ligament of the spine (OPLL). *Hum. Genet*. 104: 492–497. [Medline] [CrossRef]
30. Okamoto, K., Kobashi, G., Washio, M., Sasaki, S., Yokoyama, T., Miyake, Y., Sakamoto, N., Ohta, K., Inaba, Y., and Tanaka, H. 2004. Dietary habits and risk of ossification of the posterior longitudinal ligaments of the spine (OPLL); findings from a case-control study in Japan. *J. Bone Miner. Metab*. 22: 612–617. [Medline] [CrossRef]
31. Okawa, A., Nakamura, I., Goto, S., Moriya, H., Nakamura, Y., and Ikegawa, S. 1998. Mutation in Npps in a mouse model of ossification of the posterior longitudinal ligament of the spine. *Nat. Genet*. 19: 271–273. [Medline] [CrossRef]
32. Okawa, A., Goto, S., and Moriya, H. 1999. Calcitonin simultaneously regulates both periosteal hyperostosis and trabecular osteopenia in the spinal hyperostotic mouse (*twy*/*twy*) in vivo. *Calcif. Tissue Int*. 64: 239–247. [Medline] [CrossRef]
33. Rebbe, N.F., Tong, B.D., Finley, E.M., and Hickman, S. 1991. Identification of nucleotide pyrophosphatase/alkaline phosphodiesterase I activity associated with the mouse plasma cell differentiation antigen PC-1. *Proc. Natl. Acad. Sci. USA* 88: 5192–5196. [Medline] [CrossRef]
34. Ren, Y., Liu, Z.Z., Feng, J., Wan, H., Li, J.H., Wang, H., and Lin, X. 2012. Association of a BMP9 haplotype with ossification of the posterior longitudinal ligament (OPLL) in a Chinese population. *PLoS ONE* 7: e40587. [Medline] [CrossRef]
35. Rogers, D.C., Jones, D.N., Nelson, P.R., Jones, C.M., Quilter, C.A., Robinson, T.L., and Hagan, J.J. 1999. Use of SHIRPA and discriminant analysis to characterise marked differences in the behavioural phenotype of six inbred mouse strains. *Behav. Brain Res*. 105: 207–217. [Medline] [CrossRef]
36. Rutsch, F., Ruf, N., Vaingankar, S., Toliat, M.R., Suk, A., Hohne, W., Schauer, G., Lehmann, M., Roscioli, T., Schnabel, D., Epplen, J.T., Knisely, A., Superti-Furga, A., McGill, J., Filippone, M., Sinaiko, A.R., Vallance, H., Hinrichs, B., Smith, W., Ferre, M., Terkeltaub, R., and Nurnberg, P. 2003. Mutations in ENPP1 are accociated with 'idiopathic' infantile arterial calcification. *Nat. Genet*. 34: 379–381. [Medline] [CrossRef]
37. Rutsch, F., Vaingankar, S., Johnson, K., Goldfine, I., Maddux, B., Schauerte, P., Kalhoff, H., Sano, K., Boisvert, W.A., Superti-Furga, A., and Terkeltaub, R. 2001. PC-1 nucleoside triphosphate pyrophosphohydrolase deficiency in idiopathic infantile arterial calcification. *Am. J. Pathol*. 158: 543–554. [Medline] [CrossRef]
38. Saito, T., Shimizu, Y., Hori, M., Taguchi, M., Igarashi, T., Fukumoto, S., and Fujitab, T. 2011. A patient with hypophosphatemic rickets and ossification of posterior longitudinal ligament caused by a novel homozygous mutation in ENPP1 gene. *Bone* 49: 913–916. [Medline] [CrossRef]
39. Sakamoto, M., Hosoda, Y., Kojimahara, K., Yamazaki, T.,

and Yoshimura, Y. 1994. Arthritis and ankylosis in *twy* mice with hereditary multiple osteochondral lesions: with special reference to calcium deposition. *Pathol. Int*. 44: 420–427. [Medline] [CrossRef]

40. Sakou, T., Matsunaga, S., and Koga, H. 2000. Recent progress in the study of pathogenesis of ossification of the posterior longitudinal ligament. *J. Orthop. Sci*. 5: 310–315. [Medline] [CrossRef]
41. Schmidt, M.H., Quinones-Hinojosa, A., and Rosenberg, W.S. 2002. Cervical myelopathy associated with degenerative spine disease and ossification of the posterior longitudinal ligament. *Semin. Neurol*. 22: 143–148. [Medline] [CrossRef]
42. Takabayashi, S., Iwashita, S., Hirashima, T., and Katoh, H. 2007. The novel tetratricopeptide repeat domain 7 mutation, Ttc7fsn-Jic, with deletion of the TPR-2B repeat causes severe flaky skin phenotype. *Exp. Biol. Med (Maywood)*. 232: 695–699. [Medline]
43. Takabayashi, S., Yamauchi, Y., Tsume, M., Noguchi, M., and Katoh, H. 2009. A spontaneous smc1b mutation causes cohesin protein dysfunction and sterility in mice. *Exp. Biol. Med. (Maywood)*. 234: 994–1001. [Medline] [CrossRef]
44. Takabayashi, S. and Katoh, H. 2011. Sex identification using the ZFX and ZFY genes in Common Marmosets (*Callithrix jacchus*). *Exp. Anim*. 60: 417–420. [Medline] [CrossRef]
45. van Driel, I.R. and Goding, J.W. 1987. Plasma cell membrane glycoprotein PC-1: primary structure deduced from cDNA clones. *J. Biol. Chem*. 262: 4882–4887. [Medline]
47. Wang, H., Liu, D., Yang, Z., Tian, B., Li, J., Meng, X., Wang, Z., Yang, H., and Lin, X. 2008. Association of bone morphogenetic protein-2 gene polymorphisms with susceptibility to ossification of the posterior longitudinal ligament of the spine and its severity in Chinese patients. *Eur. Spine. J*. 17: 956–964. [Medline] [CrossRef]